

Structural Vulnerability of Energy Distribution Systems; Incorporating Infrastructural Dependencies

Arild Helseth, Arne T. Holen
Department of Electric Power Engineering
The Norwegian University of Science and Technology (NTNU)
Trondheim, Norway
helseth@elkraft.ntnu.no

Abstract—In this paper a method for assessing the structural vulnerability of two coupled energy distribution systems is proposed. The co-existing of an electric power distribution system and a district heating system is described and modelled, under the assumption that the operation of the district heating system is directly dependent on electric power. The structural vulnerability of the two systems subject to single failures or a set of simultaneous failures in the power system is found. Thus, the consequences of power system failures for the energy supply as a whole are quantified.

Index Terms—Power distribution, district heating, vulnerability, reconfiguration, network constraints, genetic algorithms (GAs), linear programming

I. INTRODUCTION

Reliability analysis of electric power systems is a rather mature field of study, covering all essential parts of the system [1], [2]. Analysing simultaneous failures in addition to single failures at distribution level will normally not significantly influence the reliability indices, due to low probability of occurrence and modest increase in consequences. Thus, most methods for reliability analysis of distribution systems focus on single failures.

On the other hand, simultaneous failures may be a result of extraordinary circumstances – such as adverse weather, malicious attacks and loss of supporting infrastructures – and will challenge the use of both human and equipment resources. The occurrence of simultaneous failures are not easily predicted and the use of generic failure rates and repair times may not be appropriate for analysing the system impact of these. In this work we emphasise on finding the consequences of multiple simultaneous failures, leaving considerations on probability of occurrence and duration of such failure sets to the judgement of the analyst.

Interruptions of electricity supply may also degrade the performance of parallel energy infrastructures, e.g. district heating and natural gas systems, which are more or less dependent on electricity for proper operation. Consequently, in order to capture the consequences of power system failures for the energy supply as a whole, these parallel infrastructures and their links to the power system should be modelled.

In this paper a method for assessing the structural vulnerability of two coupled energy distribution systems is proposed. The overall aim is to find the vulnerability of the energy

system as a whole to single or simultaneous failures in the power system. The structural vulnerability of the systems with respect to failures in the power system is defined as the consequences caused in both systems. Thus, the concept of vulnerability, as defined here, is not related to the probability of such failure sets to occur.

Several recent studies have addressed the concept of vulnerability in electric power systems, ranging from graph theoretical investigations in [3]–[5] to investigations based on more physical models in [6], [7]. These studies all refer to the transmission system, and there is a large gap between the applied definitions of vulnerability. In [8], the vulnerability to failures at distribution level is analysed using a network analytic approach. Here, the electrical properties of the network are neglected and vulnerability is defined as the degree of loss or damage to the system when exposed to a perturbation of a given type and magnitude.

Some studies have been conducted regarding infrastructural dependency modelling. In [9] a general overview of different kinds of interdependencies in critical infrastructures is given. A network analytic approach is presented in [10], identifying vulnerabilities in local distribution systems of electricity, natural gas and water. Furthermore, [11] and [12] describe and analyse the impact of natural-gas system reliability on electric power transmission systems.

The proposed method is described and illustrated for an electric power distribution system (EPDS) co-existing with a district heating system (DHS). The operation of the DHS is directly dependent on electricity. The following section describes the system modelling approach and the corresponding underlying assumptions for both the EPDS and DHS. Section III presents a screening strategy used for finding the most critical failure sets in the EPDS. A limited number of failure sets are fully analysed for both systems. In section IV, a simple example is elaborated, before the method is applied in a case study in section V.

II. SYSTEM MODELLING

Two simple systems, an EPDS and a DHS, are presented below, and a method suitable for finding the systems' vulnerabilities to failures in the EPDS is elaborated. Both the EPDS and the DHS are modelled as networks, comprising a set of

nodes \mathcal{N} and a set of branches \mathcal{B} , following an object-oriented modelling approach.

A. Vulnerability Measure

Various indices may be applied for quantification of consequences associated with interruption of energy supply in the two systems. In this study, the frequency and duration of interruptions are not calculated, and the consequences are simply described in terms of interrupted electric and thermal power for the EPDS and the DHS, denoted C_{EPDS} and C_{DHS} , respectively. It should be noted that other relevant system indices, e.g. indices related to the number and type of consumers having their supply interrupted could easily be incorporated in the presented method.

B. Electric Power Distribution System

Fig. 1 resembles a simple EPDS, comprising nodes 1-8 and branches b_1 - b_9 . The system serves seven load points (nodes 2-8). All branches have switches at their sending and receiving ends, see illustration in the top-right corner of Fig. 1. Branches b_3 and b_9 are load-transfer branches, having normally open switches at both ends. Node 1 represents the energy in-feed point, typically being a HV/MV substation.

Permanent branch and node failures in the EPDS have the potential to interrupt the service to load points. Generally, two distinctive types of interruptions may be classified, depending on interruption duration. Some load points will have their supply restored after a network reconfiguration, while others will have to wait for the repair of one or more of the faulted components. This study only considers the consequences caused by the latter type of interruption. Thus, an idealised system representation with instantaneous network reconfiguration is assumed.

The following assumptions were made when analysing the EPDS:

- temporary failures are not considered;
- all switchgear is fully reliable;
- upstream supply from HV/MV substations is fully reliable;
- load points are either fully supplied or not supplied at all.

Moreover, it was assumed that faulted load-point nodes will be isolated by the operation of a fuse, see illustration in Fig. 1. Thus, only power supply to that particular node will be interrupted. The further studies only consider branch failures in the EPDS.

For each failure set in the EPDS, the following steps are taken to find the system consequences C_{EPDS} :

- 1) Isolate the faulted branches by using the available switches
- 2) Run a Genetic Algorithm (GA) to find the optimal use of switches to minimise C_{EPDS} subject to the following constraints:
 - a) nodal voltages are not lower than a predefined minimum value at load nodes i ; $\forall i \in \mathcal{N} : V_i \geq V_{min}$
 - b) branch thermal limits are not exceeded for any branch b ; $\forall b \in \mathcal{B} : I_b \leq I_{b,max}$

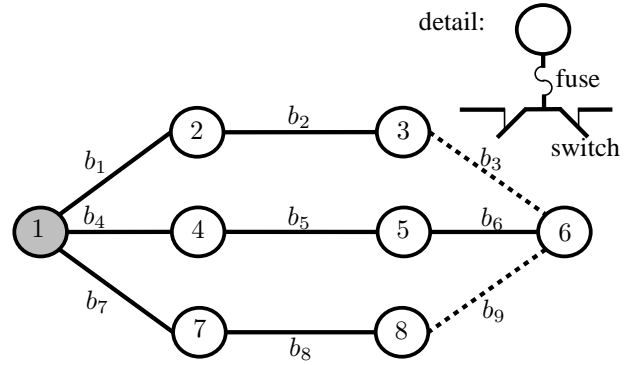


Fig. 1. A simple electric power distribution system.

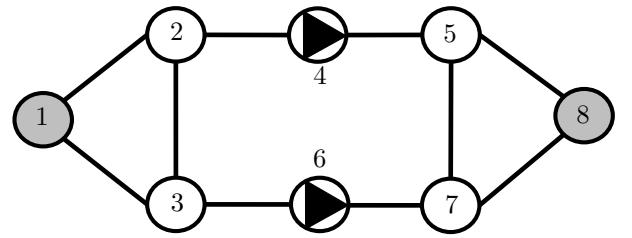


Fig. 2. A simple district heating system.

- c) the system is radially operated

The GA was modelled using the simple genetic algorithm, thoroughly described in [13], from the library GALib [14].

C. District Heating System

A simple DHS is presented in Fig. 2, comprising the following nodes; two thermal power production units (nodes 1 and 8), two pumps (nodes 4 and 6) and four load points (nodes 2, 3, 5 and 7). The system is operated as a meshed system, i.e. water may flow in all pipelines in Fig. 2.

It is possible to formulate the thermal power flow in a DHS as a function of network temperatures and pressures. In order for the system to satisfy consumers' needs, water with adequate temperature and pressure must be circulated to the load points.

In this study, only DHS node failures caused by loss of supply from the EPDS are analysed. DHS pipelines and valves are assumed fully reliable whenever the EPDS has faulted components. Losing electric power supply to nodes in the DHS may result in insufficient circulating pressure and/or insufficient thermal power production, which in turn may cause interruption of supply to DHS load points. Note that short interruptions of electric power supply to DHS nodes are not treated here, as EPDS reconfiguration is assumed to take place instantaneously. Short electric power interruptions have the potential to trip DHS pumps leading to thermal power interruptions. However, this kind of analysis calls for dynamic system studies and is outside the scope of this paper.

Pressure and temperature distribution studies may be decoupled and performed separately. Changes in pressure are quickly

transferred throughout the whole system, typically taking only a few seconds. Temperature changes are slower and closely related to the speed of the circulating water. However, as this study is not concerned with the duration of interruptions, we do not differentiate between the interruptions caused by lack of pumping capacity and those caused by lack of thermal power production capacity. It is generally assumed that repair of faulted components in the EPDS is slower than the dynamic response of the DHS. Thus, only steady-state considerations of thermal power flow are dealt with in this work.

It is assumed that all DHS nodes can be isolated and bypassed. Consequently, in case a thermal power production unit or pump lacks supply from the EPDS, the hot water is simply bypassed this unit without any increase in temperature or pressure. Furthermore, in case load has to be curtailed in the DHS due to a deficit in thermal power production or pumping capacity, it is assumed possible to bypass any load point in the system. Depending on which node types that are without electric power, different types of analysis are performed, as described below:

1) *DHS pump*: If supply from the EPDS to a DHS pump is lost, the pump is bypassed and load points in the DHS will experience a drop in pressure. An initial study of pressure distributions reveals whether load point pressures are sufficient, i.e. higher than a predefined minimum value p_{min} . If this constraint is not met, load has to be disconnected. A GA is initiated for the purpose of minimising the consequences (C_{DHS}) of load curtailment in the DHS while meeting the pressure requirement.

2) *DHS production unit*: If supply from the EPDS to a DHS thermal power production unit is lost, a capacity deficit may occur in the DHS. Rerouting of thermal power flow may also enforce bottlenecks in the DHS. The thermal power flow problem is formulated as a mixed integer programming (MIP) problem using the linear programming library GLPK [15]. The formulation relies on a lossless, steady-state network flow model. The problem formulation is stated as:

MIN.:

$$C_{DHS} = \sum_{i \in \mathcal{N}} (1 - x_i) D_i \quad (1a)$$

S.T.:

$$\sum_{j:(ji) \in \mathcal{B}} P_{b(j,i)}^t - \sum_{j:(ij) \in \mathcal{B}} P_{b(i,j)}^t + G_i - x_i D_i = 0 \quad (1b)$$

$$|P_b^t| \leq P_{b,max}^t \quad (1c)$$

$$G_i \leq G_{i,max} \quad (1d)$$

Where x_i is a boolean variable indicating whether load point i is served or not, and C_{DHS} denotes the total amount of interrupted thermal power. Restriction (1b) describes the nodal thermal-power balance for each node i , where \mathcal{B} is the collection of all branches in the DHS, $P_{b(i,j)}^t$ denotes thermal power flow in branch b connecting nodes i and j , and G_i and

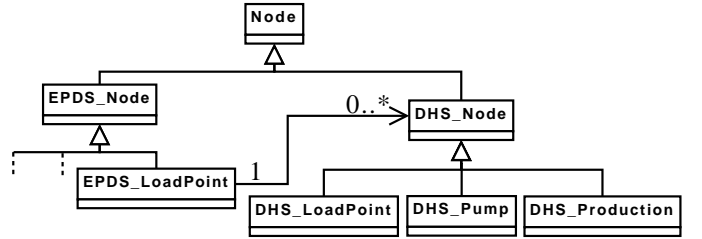


Fig. 3. Class diagram illustrating the node hierarchy.

D_i are the thermal power production and demand at node i , respectively. Restriction (1c) forces the thermal power flow in each branch not to exceed the capacity constraint $P_{b,max}^t$ for that branch. G_i is constrained by its maximum power $G_{i,max}$ in (1d).

3) *DHS load point*: Normally the DHS will interface with aggregated load points through a heat exchanger, and water is circulated in an underlying secondary circuit supplying smaller loads. Losing electric power at this location will disable the circulating pumps in the secondary circuit, and consequently the entire aggregated load point will be interrupted. However, the surrounding system is not directly affected by such local effects.

D. Modelling Dependencies

Fig. 3 shows an excerpt of the Unified Modelling Language (UML) class diagram for the node hierarchy applied in the joint modelling of the two systems. Instance variables and functions are omitted for brevity.

Each node in the DHS (DHS Node) has a link to one load point in the EPDS (EPDS LoadPoint) in Fig. 3. Each EPDS load point has an association to zero, one or several DHS nodes. DHS nodes comprise load (DHS LoadPoint), pump (DHS Pump) and production unit (DHS Production) nodes. In case an EPDS load point experiences an interruption, the model checks for associated DHS nodes. If associated DHS nodes are found, the consequences are analysed depending on the type of faulted DHS node(s), as previously described.

III. FAILURE SET SYNERGY

Applying the presented method to large scale infrastructures analysing higher-order failure sets is computationally intensive. A screening strategy inspired by [16] was applied in order to fully analyse only the most critical failure sets. Thus, computation time is reduced as well as the number of failure sets to evaluate after the simulation has been performed. The strategy is based on the concept of synergy, as explained below.

Consider the EPDS under study consisting of n components being subject to a failure set \mathcal{F}_i^k . The failure set is set number i of order k . The maximum number of failure sets of order k is found by (2).

$$i_{max}^k = \frac{n!}{(n-k)!k!} \quad (2)$$

In case k is larger than 1, it will be possible divide \mathcal{F}_i^k into a certain number of divisions, where each division comprises the same components as in \mathcal{F}_i^k . Consider a set of order 3, comprising components a , b and c . There are 4 possible divisions ($d_1 - d_4$) of $\mathcal{F}^3(abc)$, as shown below.

$$\mathcal{F}^3(abc) \begin{cases} d_1 : \mathcal{F}^2(ab) + \mathcal{F}^1(c), \\ d_2 : \mathcal{F}^2(ac) + \mathcal{F}^1(b), \\ d_3 : \mathcal{F}^2(bc) + \mathcal{F}^1(a), \\ d_4 : \mathcal{F}^1(a) + \mathcal{F}^1(b) + \mathcal{F}^1(c) \end{cases}$$

If \mathcal{F}_i^k gives rise to larger consequences (C_{EPDS}) than the sum of consequences in any of its divisions, \mathcal{F}_i^k is said to be synergistic. In other words; if \mathcal{F}_i^k is the minimum cut set for at least one EPDS load point, it will be synergistic. Thus, the synergy concept relates to network connectivity and reconfiguration capability of the EPDS.

It is possible to screen higher-order failure sets according to their synergy. A failure set of order k may cause large consequences, but if the failure set has no synergy, it indicates that these consequences were counted for when analysing sets of lower order. Thus, running the simulation with an increasing value of k , allows us to emphasise on the synergistic failures sets.

The screening procedure was implemented in the structural vulnerability assessment method as illustrated in Fig. 4. First, the depth of the analysis is set by choosing the highest failure-set order to be considered (k_{max}). Determining k_{max} is the choice of the analyst, depending on how many simultaneous failures that are considered feasible. For each k , i_{max}^k is found from (2). In case the failure set is synergistic and DHS nodes loose supply from the EPDS, one of the steps described in Subsections II-C1 - II-C3 is performed, depending on which DHS node types that are without electricity.

IV. EXAMPLE

In order to illustrate the proposed method, an example is presented based on the two systems shown in Figs. 1 and 2. The example is limited to EPDS branch failures only, and failure sets comprising three or less branches. As the EPDS has 9 branches, there are 129 failure sets in total. For clarity and simplicity, we assume that the EPDS is unconstrained. The DHS has no pipeline capacity constraints of type (1c), but will have to meet a pressure requirement $p_{min} = 0.9$ p.u. at all load points. All load points in both systems serve a load of 1 MW.

Fig. 5 shows the couplings between EPDS load points and DHS nodes in this example. The thermal power production units do not depend on electric power from the EPDS.

A total of 36 failure sets are synergistic; 27 third and 9 second-order sets. These synergistic sets are treated further in the DHS analysis. A plot of the resulting consequences for the EPDS (C_{EPDS}) and DHS (C_{DHS}) for the synergistic failure sets is presented in Fig. 6. Open circles indicate failure sets of second order and filled circles indicate third-order failure sets. For each circle in Fig. 6, there is a set of failure sets

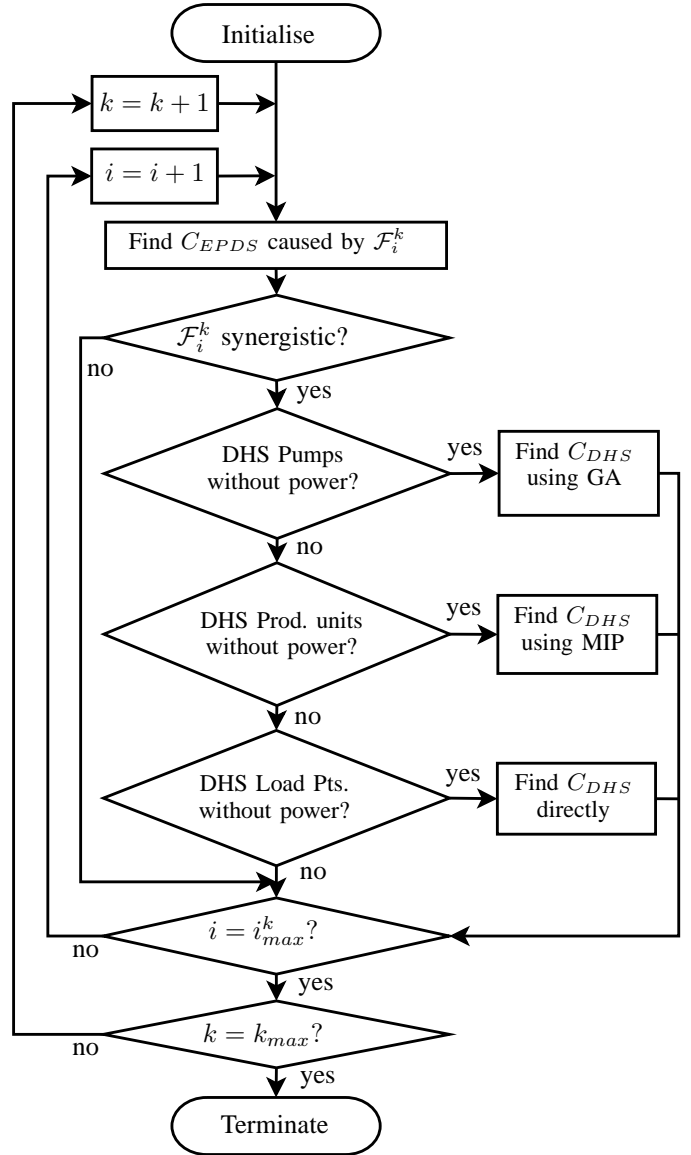


Fig. 4. Flowchart of the structural vulnerability assessment method.

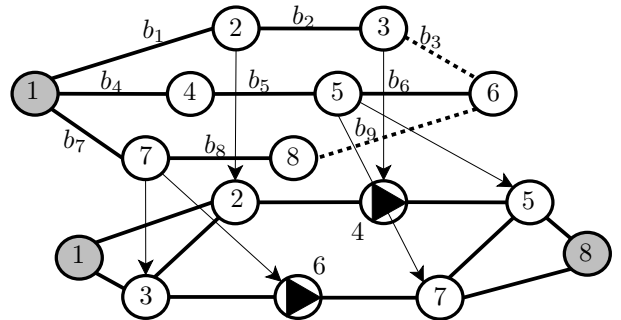


Fig. 5. Dependency of a DHS on electric power. Couplings between EPDS load points and DHS nodes are indicated by arrows.

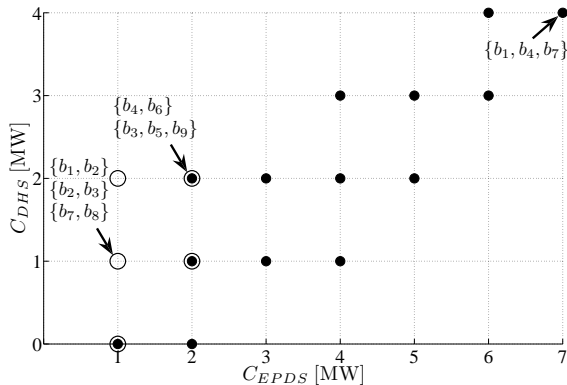


Fig. 6. Interrupted power for both the EPDS (C_{EPDS}) and the DHS (C_{DHS}). Failure sets of second order are marked with \circ and third order with \bullet .

causing this tuple of consequences. For three of these tuples, the corresponding failure sets are listed in the figure.

As an example, 3 synergistic failure sets will cause the consequence tuple of $C_{EPDS} = 1$ MW and $C_{DHS} = 1$ MW, as indicated in Fig. 6. If b_1 and b_2 fail simultaneously, EPDS node 2 will experience an interruption. According to Fig. 5, the load point at node 2 in the DHS loses supply from the EPDS and is interrupted. If b_2 and b_3 fail, EPDS node 3 will experience an interruption. This time, the DHS pump at node 4 in Fig. 2 will lose electric power supply. The GA reveals that the DHS system is only capable of serving 3 out of 4 load points in this state, thus $C_{DHS} = 1$ MW. Finally, in case b_7 and b_8 fail, both the load at node 3 and the pump at node 6 will lose power. As it is assumed that node 3 in the DHS is bypassed in this situation, the pressure constraints are not violated and no additional load points in the DHS has to be curtailed.

Simultaneous failure of b_4 and b_6 is the most critical second-order failure set in terms of total consequences ($C_{EPDS} + C_{DHS}$). Furthermore, not surprisingly, the third-order failure set comprising b_1 , b_4 and b_7 causes maximum consequences for both systems.

V. CASE STUDY

The presented method was tested on the coupled EPDS and DHS located in the city centre of Trondheim, Norway. A system boundary was defined, including only the central parts of the two systems. Figs. 7 and 8 present the structure of the two systems. It should be noted that both system models are simplified, but still reflect the basic design of the real networks.

The central part of the DHS is shown in Fig. 7. This system comprises 3 pumps, 8 thermal power production units and 11 load points, and the total installed capacity and maximum load is 149 MW and 106 MW, respectively. The surrounding EPDS is a medium-voltage cable network fed by 3 HV/MV substations and serving 34 load points. The voltage and pressure constraints were set to $V_{min} = 0.95$ p.u. and $p_{min} = 0.90$ p.u. Couplings between the two systems are mapped as in Fig. 5, but is not presented here for practical reasons.

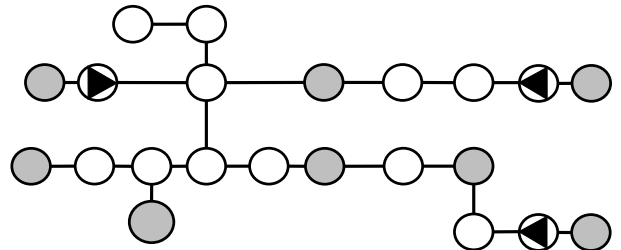


Fig. 7. Overview of the central district heating system.

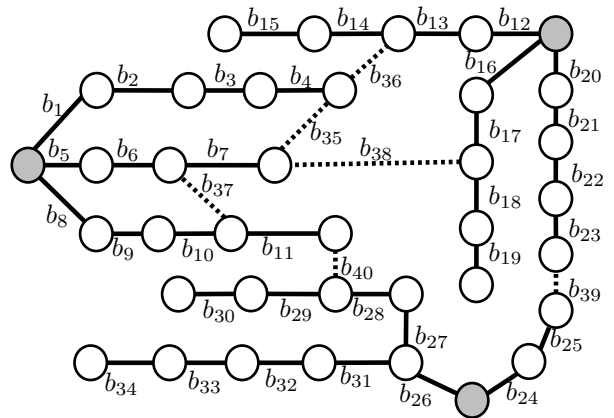


Fig. 8. Overview of the electric power distribution system. Each branch is enumerated.

A simulation was performed for failure sets comprising three or less components, considering only EPDS branch failures. In total there are 40 first, 780 second and 9880 third-order failure sets. From the simulation it was found that 12 first, 64 second and 176 third-order failure sets have synergistic consequences. A scatter plot of the consequence tuples caused by these synergistic failure sets is presented in Fig. 9. Consequences are measured in interrupted electric and thermal power, in percentage of the total load served in each of the two systems.

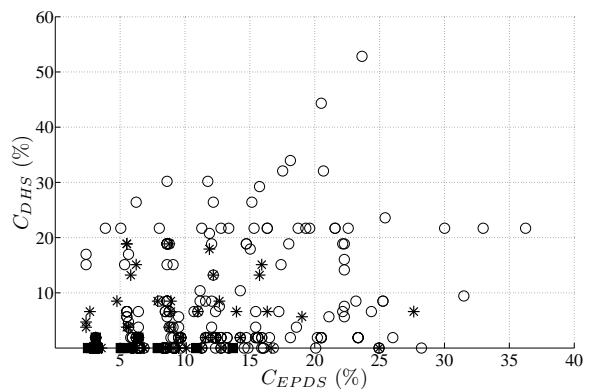


Fig. 9. Interrupted power in percentage of total load for both the EPDS (C_{EPDS}) and DHS (C_{DHS}). Failure sets of first order are marked with \blacksquare , second order with $*$ and third order with \circ .

In Table I the synergistic failure sets causing maximum consequences, both in terms of C_{EPDS} and C_{DHS} , are listed. The maximum C_{EPDS} in second and third-order synergistic failure sets was found to be 27.6 and 36.3 % of the total load in the EPDS, respectively. For comparison, the maximum C_{EPDS} in second and third-order non-synergistic failure sets was found to be 20.0 and 34.0 %.

At most 1.9 % of the DHS load is interrupted due to single branch failures in the EPDS. This result indicates that the DHS is not particularly vulnerable to single failures in the EPDS. In fact, all the major DHS load points, pumps and thermal power production units can receive power from more than one EPDS feeder.

Studying the two second-order failure sets listed in Table I, it is evident that the set causing the highest value of C_{EPDS} causes only minor consequences in the DHS. On the contrary, if branches b_5 and b_{16} fail simultaneously, violation of EPDS network constraints limits the reconfiguration capability, resulting in EPDS load point interruptions. The system is reconfigured to minimise the interrupted electric power. Cascading consequences in the DHS are not considered when finding the optimal use of switches in the EPDS. For this particular failure set a vulnerable DHS node loses electric power supply, giving a high value of C_{DHS} .

The third-order failure set comprising branches b_1 , b_{12} and b_{35} isolates a part of the EPDS which is crucial for proper DHS operation; thus, more than 50 % of the total DHS load is interrupted.

TABLE I
MAXIMUM CONSEQUENCES FOR FIRST, SECOND AND THIRD-ORDER SYNERGISTIC FAILURE SETS.

Order	Maximum	Set	C_{EPDS} (%)	C_{DHS} (%)
1 st	C_{EPDS}	b_{26}	13.7	0.0
	C_{DHS}	b_{18}	0.0	1.9
2 nd	C_{EPDS}	b_{11}, b_{26}	27.6	6.6
	C_{DHS}	b_5, b_{16}	8.8	18.9
3 rd	C_{EPDS}	b_8, b_{26}, b_{37}	36.3	21.7
	C_{DHS}	b_1, b_{12}, b_{35}	23.6	52.8

Although the non-synergistic failure sets are screened out, a thorough interpretation of the remaining synergistic failure sets \mathcal{F}_{syn} can be tedious. Finding the EPDS branches contributing the most to consequences in \mathcal{F}_{syn}^k of a given order k , will provide a measure of component criticality. The contribution R to consequences C (C_{EPDS} or C_{DHS}) of branch b is defined as the ratio between the sum of the consequences caused by synergistic failure sets including branch b and the sum of consequences for all synergistic failure sets:

$$R(b, k) = \frac{\sum_{\mathcal{F} \in \mathcal{F}_{syn}^k, b \in \mathcal{F}} [C(\mathcal{F})]}{\sum_{\mathcal{F} \in \mathcal{F}_{syn}^k} [C(\mathcal{F})]}$$

Table II shows the three components that contributed the most to consequences (in terms of C_{EPDS} and C_{DHS}) caused by second-order synergistic failure sets.

TABLE II
BRANCH CONTRIBUTION TO CONSEQUENCES IN SECOND-ORDER SYNERGISTIC FAILURE SETS.

Rank	$C = C_{EPDS}$		$C = C_{DHS}$	
	Branch (b)	Contr. (R)	Branch (b)	Contr. (R)
1	b_{26}	0.090	b_{16}	0.115
2	b_{24}	0.075	b_{20}	0.113
3	b_{20}	0.069	b_{21}	0.076

VI. DISCUSSION

In this study, the frequencies and durations of interruptions were not considered, only the system consequences in terms of interrupted electric and thermal power. Obviously, before drawing final conclusions regarding critical components and possible system reinforcements, one has to somehow evaluate how often interruptions are expected to occur and for how long they are expected to last.

Furthermore, the assumptions regarding the two systems' responses and operations due to failures can be questioned. It is difficult to generalise such behaviour when the failure repair time is unknown. For example, losing power to a DHS thermal power production unit for a short time, leading to a short-time capacity deficit in the DHS, will rarely be noticed by the average consumer. This work relies on the assumption that electric power interruptions affecting supply to DHS nodes last longer than the time it takes for the thermal power flow to reach steady-state. More detailed system studies could address the dynamic response of the DHS subject to short electric power interruptions, and the sequence of backing up or restarting faulted pumps and production units.

In the presented method, the post-failure system configurations are found in two separate steps. First, the EPDS is reconfigured to minimise interrupted electric power by using the available switches. Subsequently, in case any DHS nodes are without power, curtailed thermal power is minimised while meeting the DHS network constraints. A perhaps more realistic reconfiguration algorithm would integrate the two reconfiguration steps in one procedure. In this way, the cascading consequences in the DHS are considered when finding the optimal use of switches in the EPDS. By integrating the system reconfigurations in this manner, it is likely to expect a reduction in C_{DHS} and a slight increase in C_{EPDS} for some failure sets. In the end, the most representative algorithm will always be the one reflecting the actual communication and cooperation between the distribution system operators.

Finally, it should be noted that simulating the EPDS as a partial system may result in a higher measure of structural vulnerability than in reality, since boundary nodes may be fed by surrounding system parts. These parts are outside the system boundary and are therefore not included in the system model.

VII. CONCLUSION

A method was proposed, suitable for analysing the structural vulnerability of an electric power distribution system co-existing with a district heating system. The structural vulnerability of these systems with respect to failures in the power system was defined as the consequences caused in both systems. The cascading consequences due to loss of electric power to essential components in the district heating system was discussed and modelled. The method enables the analyst to consider higher-order failure sets in the electric power system and find the consequences caused in both systems. Furthermore, a screening procedure was applied to identify and fully analyse only the most critical failure sets.

The method was applied to a case study, where the failure sets causing the highest consequences were identified. It was briefly discussed and shown how to rank power system components in terms of criticality.

ACKNOWLEDGEMENT

The authors would like to thank May Toril Moen and Arnvid Sylte at Trondheim Energi for interesting discussions and for providing data for the case study.

REFERENCES

- [1] J. Endrenyi, *Reliability Modeling in Electric Power Systems*. John Wiley & Sons Ltd., 1978.
- [2] R. Billinton and R. N. Allan, *Reliability Evaluation of Power Systems*, 2nd ed. Plenum Press, 1996.
- [3] R. Albert, I. Albert, and G. L. Nakarado, "Structural vulnerability of the north american power grid," *Physical review E*, vol. 69, p. 4, 2004.
- [4] P. Crucitti, V. Latora, and M. Marchiori, "A topological analysis of the italian electric power grid," *Physica A: Statistical Mechanics and its Applications*, vol. 338, pp. 92–97, 2004.
- [5] Å. J. Holmgren, "Using graph models to analyze the vulnerability of electric power networks," *Risk Analysis*, vol. 26, pp. 955–969, 2006.
- [6] G. Doorman *et al.*, "Vulnerability analysis of the nordic power system," *IEEE Transactions on Power Systems*, vol. 21, pp. 402–410, 2006.
- [7] X. Yu and C. Singh, "A practical approach for integrated power system vulnerability analysis with protection failures," *IEEE Transactions on Power Systems*, vol. 19, pp. 1811–1820, 2004.
- [8] H. Jonsson, J. Johansson, and H. Johansson, "Analysing the vulnerability of electric distribution systems: a step towards incorporating the societal consequences of disruptions," *International Journal of Emergency Management*, vol. 4, pp. 4–17, 2007.
- [9] S. M. Rinaldi, "Modeling and simulating critical infrastructures and their interdependencies," in *Proceedings of the Hawaii International Conference on System Sciences*, vol. 37, Hawaii, USA, 2004, pp. 873–880.
- [10] G. E. Apostolakis and D. M. Lemon, "A screening methodology for the identification and ranking of infrastructure vulnerabilities due to terrorism," *Risk Analysis*, vol. 2, pp. 361–376, 2005.
- [11] J. Munoz, "Natural gas network modeling for power systems reliability studies," in *Power Tech Conference*, vol. 4, Bologna, Italy, 2003.
- [12] M. Shahidehpour, Y. Fu, and T. Wiedman, "Impact of natural gas infrastructure on electric power systems," *Proceedings of the IEEE*, vol. 93, no. 5, pp. 1042–1056, 2005.
- [13] D. E. Goldberg, *Genetic Algorithms in Search, Optimization, and Machine Learning*. Reading, MA: Addison-Wesley, 1989.
- [14] M. Wall, "GALib: A C++ library of genetic algorithm components," [online]. Available: <http://lancet.mit.edu/ga/>.
- [15] A. Makhorin, "GLPK (GNU Linear Programming Kit)," [online]. Available: <http://www.gnu.org/software/glpk/glpk.html>.
- [16] H. Jonsson, J. Johansson, and H. Johansson, "Identifying critical components in electric power systems: A network analytic approach," in *Proceedings of the European Safety and Reliability Conference (ESREL)*, Stavanger, Norway, 2007.